N·H

ELSEVIER

PHYSICA E

Direct measurements of electron thermalization in Coulomb blockade nanothermometers at millikelvin temperatures

T.A. Knuuttila [a,*], K.K. Nummila [a], W. Yao [a], J.P. Kauppinen [b], J.P. Pekola [b]

[a] *Low Temperature Laboratory, Helsinki University of Technology, P.O. Box 2200, 02015 HUT, Finland*
[b] *Department of Physics, University of Jyväskylä, P.O. Box 35, 40351 Jyväskylä, Finland*

Abstract

We investigate electron thermalization of tunnel junction arrays installed in a powerful dilution refrigerator whose mixing chamber can produce lattice temperatures down to 3 mK. The on-chip Coulomb blockade thermometers (CBT) against other thermometers at the mixing chamber provide direct information on the thermal equilibrium between the electronic system and the refrigerator. We can detect and discriminate between the heat load delivered through the wiring and that produced by the bias current of the CBT-measurement. The basic heat leak limits the minimum of the electronic temperature to slightly below 20 mK. © 1998 Elsevier Science B.V. All rights reserved.

Many of the electronic microstructures and nanostructures exhibit clean quantum phenomena in their full strength only towards the lowest temperatures. An absolute method to determine the electron temperature in these structures is to use a Coulomb blockade thermometer. It is generally believed that electrons in submicron systems often cannot be cooled in equilibrium with the underlying lattice much below 100 mK. Consequently, numerous effects in "nanoelectronics" are possibly limited by incomplete thermalization of the electronic system. Examples of these include normal metal and superconducting single electron tran-

sistors and boxes for ultrasensitive electrometry and pumps for metrological current standards, to mention just a few of them [1–3]. The IV-characteristics of single electron transistors and arrays of ultra-small tunnel junctions are more smeared than expected at very low refrigerator temperatures. In single electron boxes the steps between different charge states should become extremely sharp at temperatures around 20 mK, but owing to either incomplete thermalization or to some other reasons, the shape changes only weakly below 100 mK. Similarly, the transfer accuracy of single charge pumps should improve drastically with decreasing electronic temperature, but, on the contrary, it saturates to the level corresponding to an effec-

* Corresponding author.

tive temperature of about 100 mK even in the best realizations of the effect. Therefore, it is essential to understand under which circumstances the thermal equilibrium between electrons and the substrate can be attained well below 100 mK. Another important motivation for this investigation is the lack of sensitive primary thermometers in the temperature range between 20 and 100 mK.

In a typical low temperature set-up, a mesoscopic sample is cooled in thermal contact with a dilution refrigerator capable of maintaining a minimum bath temperature of below 10 mK in the best cases. The sample is normally wired using resistive leads with thermal anchoring and high frequency filtering at various temperatures of the cryostat, like 300, 4, 1 K and 10 mK. Additionally, a metallic sample enclosure, and ground lines for wiring provide shielding against rf interference and thermal radiation. All this must be properly configured in order to reduce the external sources of heat, which tend to lift the base temperature of the electronic system of interest above that of the refrigerator. Examples of special cryo-filters comprising lithographically patterned on-chip RLC-elements or *Thermocoax* cable are given in Refs. [4, 5].

In this paper we discuss our direct measurements on thermalization of nano-fabricated tunnel junction thermometers [6–8] and demonstrate that by careful anchoring of the leads and design of the sample itself electronic temperatures below 20 mK can be achieved.

We fabricate samples by the standard two-angle evaporation of aluminum on oxidized or nitridized silicon substrates. A tunnel barrier is formed in pure oxygen at room temperature. The overlap area between the two layers determines the size and thus the capacitance of the tunnel junction. Fig. 1 shows the geometry of sample A. Additional fins were attached to the islands between the junctions to improve the thermalization of electrons at low temperatures. In sample A the junction area is $0.9\,\mu m^2$ and the volume of the island is $22.6\,\mu m^3$. In sample B they are 1.8 and $46.2\,\mu m^3$, respectively. Both samples consist of arrays of 40 junctions with four/two (sample A/B) arrays connected in parallel (not shown in Fig. 1) to reduce the total resistance.

The measurements were carried out in a nuclear demagnetization cryostat [9]. The samples were fixed to the bottom plate of the mixing chamber of the ^{3}He/^{4}He dilution refrigerator having a base temperature below
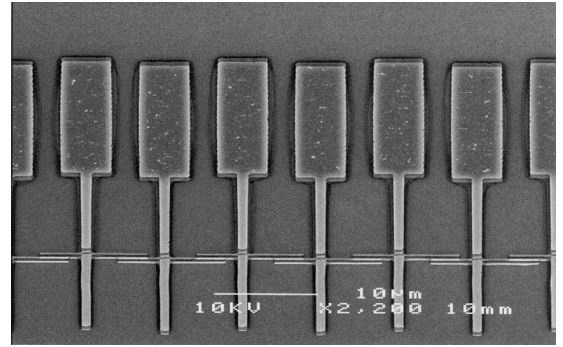

Fig. 1. A scanning electron microscope image of a section of sample A. The large pads attached to the islands are the extra fins for thermalization and the overlapping small steps in between form the junctions. The scale is shown by the $10\,\mu m$ line.

3 mK. The temperature scale was established with a primary ^{60}Co nuclear orientation thermometer below 35 mK whereas at higher temperatures, above 50 mK, a factory calibrated germanium thermometer [10] was used. In the intermediate region, temperatures were measured with a vibrating wire viscometer located inside the mixing chamber. The viscometer was also utilized for cross-checking the temperature scales of the other two thermometers. We estimate the temperature calibration to be correct within ±5% based on the consistency of all our thermometers, including a ^{195}Pt NMR thermometer.

An array of small tunnel junctions between normal metal electrodes can be used both as a primary and as a secondary thermometer. For primary thermometry, the temperature can directly be obtained from the full width of the measured conductance dip at half minimum, $V_{1/2}$, through the analytical result $eV_{1/2,0}/Nk_B T \cong 5.439$, where N is the number of junctions in the array [7] and the subscript 0 indicates that this is the high temperature limit for homogeneous arrays. At the lowest temperatures a linear correction, $(V_{1/2} - V_{1/2,0})/V_{1/2,0} \cong 0.39211\Delta G/G_T$, must be introduced to the half-width of the previous relation [8]. The inverse of the depth of the conductance curve, $(\Delta G/G_T)^{-1}$, is linear in T, such that $(\Delta G/G_T)^{-1} = [3Nk_B/(N-1)(e^2/2C)]T$, and thus acts as a secondary thermometer, once the capacitance, C, of the sample has been determined at a known temperature. At low temperatures known linear corrections can be applied to $(\Delta G/G_T)^{-1}$ as well [8].

The samples were installed in tightly sealed copper enclosures surrounded by small coils used to generate magnetic fields in order to suppress the superconductivity of the Al electrodes. Alternatively, we employed NdFeB permanent magnets to this end, but they introduced an unacceptable heat load to the thermometer below 100 mK. The wiring from room temperature down to the mixing chamber was made using thin coaxial cables with a NbTi inner conductor embedded in a CuNi matrix. The cables were thermally anchored at 4.2 K. Additionally, short sections, about 25 cm, of *Thermocoax* [5], located just before the copper enclosure and connected to the mixing chamber temperature over the whole length, were used to reduce high-frequency interference. The attenuation for the used *Thermocoax* having a diameter of 0.5 mm is as much as 200 dB/m at 20 GHz [5]. In most measurements with sample A, an LC-filter [11], at the mixing chamber temperature, was employed as well. The filter, originally designed for use with carbon resistor thermometers, was effectively a 44 nF parallel capacitance to ground. It also substantially improved the thermal anchoring of the inner conductors which otherwise were effectively anchored at 4.2 K only.

The conductance, G, versus bias voltage curves were measured by slowly sweeping a DC-current over the full bias range with a small, typically 30 Hz AC-modulation added. A typical sweep time was 20 min and the AC-excitation was always kept sufficiently small, $\leqslant 5\%$ of $V_{1/2}$ (full width at half minimum). There is a systematic error both in $V_{1/2}$ and $\Delta G/G_{\rm T}$ due to the non-zero AC-amplitude which averages the differential conductance over a non-negligible bias range. These errors, however, are below 1% with a 10% excitation level. At the lowest temperatures, the relative drop of conductance at zero bias, $\Delta G/G_{\rm T}$, was measured with a very narrow DC-sweep just over the region of the minimum in order to reduce the ohmic heating caused by the bias voltage, while $G_{\rm T}$ of the asymptotic region was obtained from a wider sweep. Further in the $\Delta G/G_{\rm T}$ measurements with the LC-filter, the AC-modulation of 2 Hz was necessary, owing to the low cut-off frequency.

Fig. 2 shows the temperatures indicated by the two primary tunnel junction thermometers plotted against the calibration temperature. The estimated error in $T_{\rm CBT}$, due to noise in the measurement and data fitting, is $\leqslant 5\%$. At the high temperature end the agree-
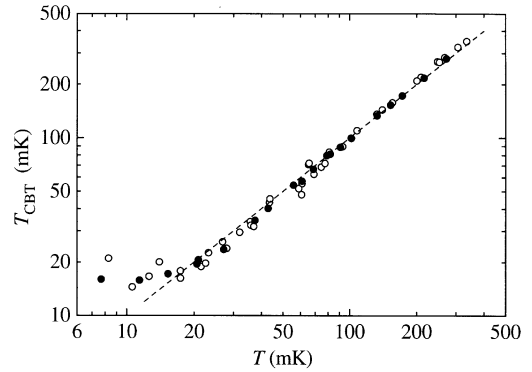

Fig. 2. CBT-temperature deduced from $V_{1/2}$ versus the calibration temperature. Open and closed circles refer to samples A and B, respectively. The dashed line shows the ideal one-to-one behavior.

ment is well within the error limits. At intermediate temperatures, from 80 to 20 mK, $T_{\rm CBT}$ drops slightly below the ideal behavior. Below 20 mK, the tunnel junctions saturate and do not follow the temperature anymore. The data for sample A were measured with the LC-filter. After the filter was removed the sample A clearly saturated at a higher temperature (data not shown).

Heating through the measurement wires most probably causes the saturation of the junction temperature. We estimate the thermal resistance of the CuNi matrix from 4.2 K down to mixing chamber to be 2×10^9 K^2/W, while for the *Thermocoax* we obtain 5×10^8 K^2/W. This gives an upper limit of 3.2 nW heating to the soldering pads at the ends of the sample-array. The dominating thermal resistance between the pads and the mixing chamber is the silicon substrate as has been argued in Ref. [12]. Taking a thermal conductivity of the form $\kappa = aT^b$, with $a = 6.4$ W/mK$^{3.68}$ and $b = 2.68$ [13] and using the estimated heat leak, we obtain a temperature difference of 10 mK over the substrate thickness of 0.5 mm at 20 mK. Thus the lower saturation temperature of sample A in measurements with the filter in place is probably owing to better thermal anchoring of the inner conductors in the filter enclosure at the mixing chamber temperature.

The bias current induces Joule heating in the tunnel junctions which can be observed as changes in the line shape. The observed drop of $T_{\rm CBT}$ below the ideal behavior in Fig. 2 is due to this effect, which makes the tip of the conductance dip narrower and broadens the wings, as shown in the inset of Fig. 3 for a conduc-
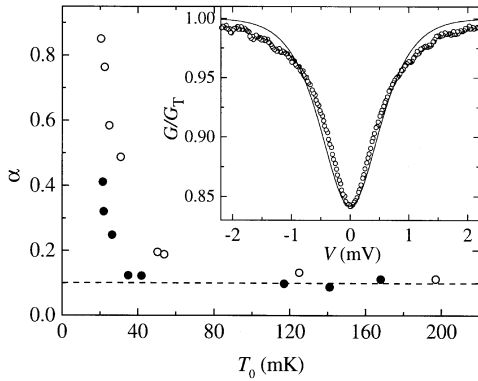
Fig. 3. Bias heating as a function of temperature. The increase of the α parameter with decreasing temperature is due to bias heating. Open and closed circles refer to samples A and B, respectively. Negligible bias heating corresponding to $\alpha = 0.1$ is indicated by the horizontal dashed line. Inset: Measured G/G_T of sample A at 59 mK as a function of DC-bias voltage. The solid line shows the ideal theoretical behavior, obtained from numerical calculations.
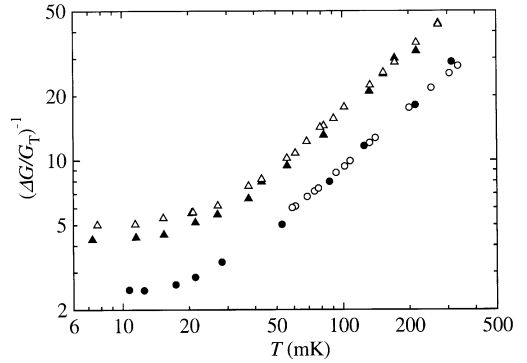

Fig. 4. Inverse of $\Delta G/G_T$ as a function of temperature. Circles denote data measured with sample A and triangles with sample B, whereas open and closed symbols refer to measurements performed with full and narrow DC-sweeps, respectively.

tance curve measured at 59 mK. We analyze the bias heating by fitting the low bias range of the conductance curves to a parabolic form $G/G_T = 1 - \Delta G/G_T(1 - \alpha v^2)$, with α as the fit parameter [12]. For perfect thermalization $\alpha = 0.1$. Here $v = eV/Nk_B T_0$ where T_0 is the temperature deduced from $\Delta G/G_T$ at $V = 0$, i.e. at zero bias heating. The conductance curves were measured with a narrow DC-sweep covering about $\pm 5\%$ of $V_{1/2}$. The results of the fits are shown in Fig. 3. The tip of the conductance curve narrows with decreasing temperature leading to an increase in α. It can be seen that in sample B, with larger cooling pads, the bias heating shows up at lower temperatures. The data allow us to estimate the electron phonon coupling parameter [12, 14, 15]. For sample A we get $\Sigma \approx 0.1$ nW/K$^5\mu$m^3.

$(\Delta G/G_T)^{-1}$ versus temperature is plotted in Fig. 4 for the two samples. The capacitance values, obtained by fitting to the high temperature ends, are 26.3 and 52.7 fF, for samples A and B, respectively. These values agree very well with the known areas of the junctions. The behavior is linear at the high temperature end, but saturates in the same temperature range as $V_{1/2}$, even with the narrow DC-sweep measurements. This further suggests that bias heating is not the cause of saturation. The data for sample A were measured with the filter, in contrast to sample B, and should thus have shown a lower saturation temperature, but unfortunately, for sample A, temperatures below 25 mK

are in a region where background charge effects are supposed to limit the performance [8].

In conclusion, we have investigated electron thermalization in normal tunnel junction arrays at millikelvin temperatures. Our results show that thermal equilibrium between the electrons and the substrate can be maintained to slightly below 20 mK. Coulomb blockade thermometers can thus be used for both primary and secondary thermometry down to these temperatures. Further, we believe that the saturation temperature, especially, in measurements employing narrow DC-sweeps over the conductance minimum, can still be lowered by more careful thermal anchoring of the wires.

Acknowledgements

References

[1] D. Esteve, in: H. Grabert, M.H. Devoret (Eds.), Single Charge Tunneling, Coulomb Blockade Phenomena in Nanostructures, Plenum Press, New York, 1992, p. 109.
[2] H. Pothier, Ph.D. Thesis, unpublished, Saclay, France, 1991.
[3] M.W. Keller, J.M. Martinis, N.M. Zimmerman, A.H. Steinbach, Appl. Phys. Lett. 69 (1996) 1804.

[4] D. Vion, P.F. Orfila, P. Joyez, D. Esteve, M.H. Devoret, J. Appl. Phys. 77 (1995) 2519.

[5] *Thermocoax* manufactured by Philips. Its use for filtering in cryoelectronic experiments has been discussed in A.B. Zorin, Rev. Sci. Instrum. 66 (1995) 4296.

[6] J.P. Pekola, K.P. Hirvi, J.P. Kauppinen, M.A. Paalanen, Phys. Rev. Lett. 73 (1994) 2903.

[7] K.P. Hirvi, J.P. Kauppinen, A.N. Korotkov, M.A. Paalanen, J.P. Pekola, Appl. Phys. Lett. 67 (1995) 2096.

[8] Sh. Farhangfar, K.P. Hirvi, J.P. Kauppinen, J.P. Pekola, J.J. Toppari, D.V. Averin, A.N. Korotkov, J. Low Temp. Phys. 108 (1997) 191.

[9] W. Yao, T.A. Knuuttila, J.E. Martikainen, K.K. Nummila, A.S. Oja, O.V. Lounasmaa, unpublished.

[10] GR-200A-30, Manufactured by Lake Shore Cryotronics Inc., 64 East Walnut Street Westerville, Ohio 43081-2399, U.S.A., calibration date March 31, 1995.

[11] F. Pobell, Matter and Methods at Low Temperatures, Springer, Berlin, 1992, p. 232.

[12] J.P. Kauppinen, J.P. Pekola, Phys. Rev. B 54 (1996) R8353.

[13] S.M. Sze, Physics of Semiconductor Devices, Wiley, Singapore, 1981.

[14] M.L. Roukes, M.R. Freeman, R.S. Germain, R.C. Richardson, M.B. Ketchen, Phys. Rev. Lett. 55 (1985) 422.

[15] F.C. Wellstood, C. Urbina, J. Clarke, Phys. Rev. B 49 (1994) 5942.